Diamond-Like Carbon Films

Subjects: Materials Science, Coatings & Films | Transportation

Contributor: Naoto Ohtake

Diamond-like carbon (DLC) films have been extensively applied in industries owing to their excellent characteristics such as high hardness. In particular, there is a growing demand for their use as protective films for mechanical parts owing to their excellent wear resistance and low friction coefficient. DLC films have been deposited by various methods and many deviate from the DLC regions present in the ternary diagrams proposed for sp^3 covalent carbon, sp^2 covalent carbon, and hydrogen. Consequently, redefining the DLC region on ternary diagrams using DLC coatings for mechanical and electrical components is urgently required. Therefore, we investigate the sp^3 ratio, hydrogen content, and other properties of 74 types of amorphous carbon films and present the classification of amorphous carbon films, including DLC. We measured the sp^3 ratios and hydrogen content using near-edge X-ray absorption fine structure and Rutherford backscattering-elastic recoil detection analysis under unified conditions. Amorphous carbon films were widely found with nonuniform distribution. The number of carbon atoms in the sp^3 covalent carbon without bonding with hydrogen and the logarithm of the hydrogen content were inversely proportional. Further, we elucidated the DLC regions on the ternary diagram, classified the amorphous carbon films, and summarized the characteristics and applications of each type of DLC.

carbon diamond-like carbon classification sp3 hybridization sp2 hybridization

1. Introduction

Diamond-like carbon (DLC) films are a kind of amorphous carbon film, wherein both the σ and π bonds due to sp^3 and sp^2 hybrid orbitals constituting diamond and graphite, respectively, are the carbon skeletons [1][2][3][4]. Aisenberg and Chabot conducted a series of experiments to fabricate diamond films using a carbon ion beam and confirmed the formation of diamond-like amorphous carbon films, known as diamond-like carbon. This marked the beginning of DLC research [5].

DLC films feature high hardness, high wear resistance, low friction coefficient, high insulation, high chemical stability, high gas barrier properties, high anti-burning properties, high biocompatibility, and high infrared permeability. DLC films with flat surfaces can be synthesized at low temperature (~200 °C). Hence, they have a wide range of applications [6][7][8], such as electric and electronic equipment (e.g., hard disks, video tapes, integrated circuits), cutting tools (e.g., drills, end mills, razors), molds (e.g., optical parts, injection molding), automotive parts (e.g., piston rings, cam-related parts, clutch plates, pumps, injectors), optical components (e.g., lenses), plastic bottle oxygen barrier films, sanitary equipment (faucets), windows, bathtub mirrors, and decorative items. Their demand as protective films for automotive parts is rapidly increasing, particularly due to their excellent wear resistance and low friction coefficient properties [9].

The ratio of sp^3 to sp^2 binding in DLC ranges from ~10% to ~90%. Moreover, the hydrogen content in DLC varies from 0 to 50 at%. Robertson et al. proposed a ternary diagram [10] of sp^3 carbon, sp^2 carbon, and hydrogen targeting DLC films with large chemical bonding and compositional variations, which provides the understanding of DLC existence regions in the sp^3 bond, sp^2 bond, and hydrogen content axes. The diagram was constructed using 28 sets of experimental data referenced by Robertson et al. All the samples were evaluated by nuclear magnetic resonance (NMR) and elastic recoil detection analysis (ERDA). Jacob et al. proposed a fully constrained network model [11][12] on this ternary diagram to demonstrate the degree of clustering of the sp^2 phase shown as a region. Furthermore, the DLC film is classified based on the sp^3 ratio and hydrogen content cited by 19 studies [13]. Bewilogua et al. [14] and Reinke et al. [15] strengthened the diagrams by adding experimental data on the sp^3 ratio of hydrogenated amorphous carbon films obtained from Fourier-transform infrared spectroscopy (FTIR) spectra and confirmed that hydrocarbon films can be classified into two types, regardless of the production method. Zhang et al. created a ternary diagram comprising nanocrystalline graphite, a fused aromatic ring, and olefinic chain clusters from a survey of the Raman spectra of many DLC films; further, they classified DLC primarily based on the morphology characterized by the presence of sp^2 carbons [16].

To date, Vetter investigated and detailed the addition of various additives (e.g., Si, F, B, Ti, Al, Mo, Co, Fe, Ni, Cu, W, Zr, Ag, Au, H, and N) in DLC films. Notably, the static contact angle of a water droplet and electric properties of DLC vary significantly, depending on the type and concentration of the third element added [17]. The film structure forms a mixing layer, which lowers the sp^3 ratio near the substrate or forms an intermediate layer. The amorphization trajectory of the sp^2 phase clustering, which ranges from crystalline graphite to amorphous carbon, has been explained by a model that changes from nanocrystalline graphite with a cluster size of ≥2 nm to a fused aromatic ring of ≤2 nm and further converts it into olefin-chain nanoclusters [18][19]. The hydrogen content in DLC films significantly impacts both the hardness and friction coefficient. Furthermore, the friction coefficient of DLC films grown using raw material gas with a very high hydrogen/carbon ratio (e.g., 10) is typically very low (μ = 0.003), whereas that of DLC films without hydrogen is very high (μ = 0.65) [20].

Amorphous carbon films containing DLC films are synthesized by various methods such as chemical vapor deposition (CVD), which includes plasma-enhanced CVD [21][22][23][24][25][26][27][28][29], electron cyclotron resonance (ECR) plasma CVD [30], plasma-based ion implantation and deposition (PBII&D) [31][32], and physical vapor deposition, which includes ionized evaporation [33], sputtering [34][35], unbalanced magnetron sputtering (UBMS) [36][37], ECR sputtering [38][39], high-power impulse magnetron sputtering (HiPIMS) [40][41], filtered cathodic vacuum arc (FCVA) [42][43][44][45], ion-beam deposition (IBD) [5][46][47][48], arc ion plating (AIP) [49][50], pulsed laser deposition (PLD) [51], and laser arc deposition [52][53]. Many of the DLC films produced by these methods have deviated from the DLC regions on the ternary diagrams reported to date. Therefore, redefining the DLC region on the ternary diagram, which uses DLC coatings for mechanical and electrical components, is urgently required in academia and industries. In fact, Germany made a national effort to standardize the carbon films and published the German standard VDI2840 in 2005 [54].

Therefore, in this study, 74 types of amorphous carbon films were collected, and the sp^3 ratios and hydrogen contents of the films were evaluated. Importantly, the properties of the amorphous carbon films were each

evaluated using a single near-edge X-ray absorption fine structure (NEXAFS) for the sp^3 ratio analysis, a single ^{13}C NMR for the sp^3 ratio analysis, and a single Rutherford backscattering spectroscopy-ERDA (RBS-ERDA) for the hydrogen content analysis, to eliminate errors due to differences in the equipment and measurement conditions. The DLC regions were clarified on the ternary diagram based on the measured data. Subsequently, the amorphous carbon films containing DLC were classified.

The effects of sp^3 ratio and hydrogen content on various properties of amorphous carbon were clarified by comparing and investigating the results of the sp^3 ratio and hydrogen content obtained by RBS-ERDA with those of the density, refractive index, extinction coefficient, nano-indentation hardness, visible light Raman spectrum, ultraviolet light Raman spectrum, static water-drop contact angle, and corrosion properties. Finally, the type of DLC film and its application fields were described based on the classification results and characteristic evaluation of amorphous carbon films.

2. DLC Characteristics and Applications

Figure 11 summarizes the classification of amorphous carbon films by making the plots on a ternary diagram. Although this classification was similar to that summarized by Robertson et al. [10], a clearer classification using data from 74 types of amorphous carbon analyzed in a single series by the same analyzer was achieved. In general, ta-C films are presumably free of hydrogen or have minimal amounts because, by definition, the tetrahedral structure predominantly contains σ bonds. Therefore, ta-C was considered the region where the sp^3 ratio exceeded 50% and the hydrogen content was <~5 at%. Further, a-C was classified as the region where the sp^3 ratio and hydrogen content were ≤50% and ≤5 at%, respectively. Figure 10 also depicts a clear separation between ta-C and a-C in terms of the nano-indentation hardness. The large region with an sp^3 ratio and hydrogen content of <50% and >5 at%, respectively, was labeled as a-C:H if a large amount of hydrogen was introduced into a-C. Regions where hydrogen was introduced into ta-C could be expressed as ta-C:H in a manner similar to that of a-C:H. These four regions are all DLC, which may be classified as polymer-like carbon films in the cases where the hydrogen content is high (>~40 at%) and a linear chain structure is dominant. These films also exhibit small hardness values. However, there are also films with hardness values >9 GPa, even when the hydrogen contents exceed 40 at%. These films did not adopt a linear structure and were considered as a-C:H or ta-C:H.

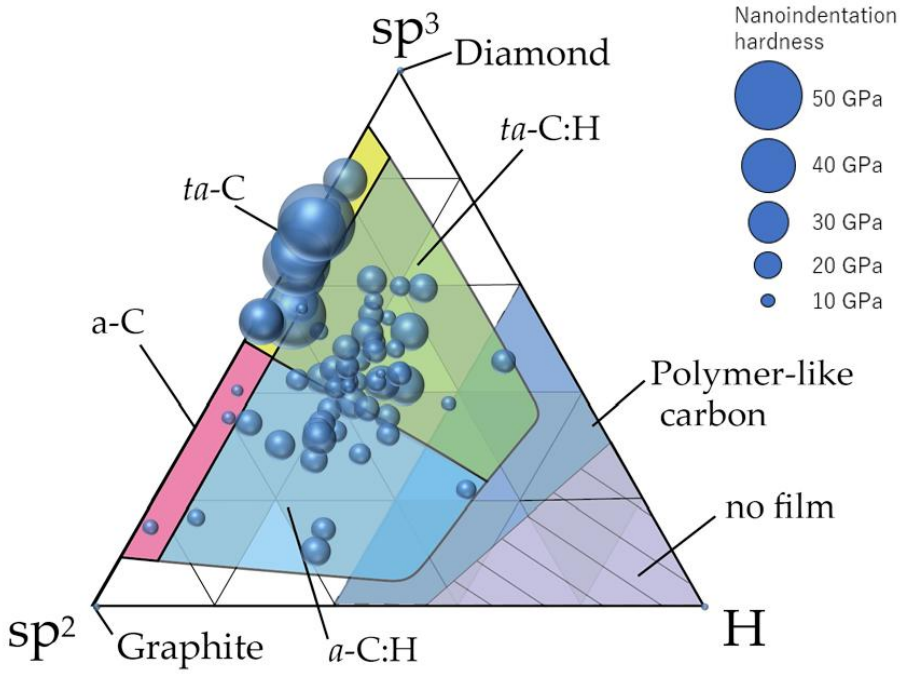

Figure 11. Distribution of 74 types of amorphous carbon films on the ternary diagram. The diameter of the circle corresponds to the nanoindentation hardness of each amorphous carbon film.

Interestingly, a gap (5–20 at%) existed where the hydrogen content was not uniformly distributed. Hence, there are very few films with hydrogen contents of 5–20%. Tetrahedral structures with sp^3 bonds as the skeleton were stabilized without hydrogen, adopting a structure with an a-C:H ratio of 3–4:1 when hydrogen is introduced into the DLC. However, it is difficult to distinctly determine this structure as the hydrogen content in the sp^3 and sp^2 domains are expected to differ [55][56].

Table 1 summarizes the characteristics of amorphous carbon films and its applications by associating the results obtained in this study with the classifications. ta-C is used for various components including mechanical parts, automotive parts, machining tools, cutting tools, metal molds, hard disk heads, infrared transmission protective films, low-dielectric-constant materials, and insulating materials due to its high hardness. ta-C:H is used for various components such as mechanical parts, automotive parts, metal molds, hard disks, magnetic tapes, optical element coatings, and scissors owing to its relatively high hardness and low friction coefficient. a-C is used for components such as optical element coating; and a-C:H is used for components such as mechanical parts, biomedical material coating, sealing materials, gas barrier coating, low-dielectric-constant materials, and insulating materials. PLC is exclusively utilized for gas barrier coatings.

Table 1. Classification of amorphous carbon films including DLC films, and those with industrial applications.

Classification	DLC	DLC	DLC	DLC	not DLC
Short name	ta-C	ta-C:H	a-C	a-C:H	PLC

Classification	DLC	DLC	DLC	DLC	not DLC
Designation	Tetrahedral hydrogen-free amorphous carbon film	Tetrahedral hydrogenated amorphous carbon film	Hydrogen-free amorphous carbon film	Hydrogenated amorphous carbon film	Polymer-like carbon
$sp^3/(sp^3 + sp^2)$ (%)	50–90	50–90	10–50	10–50	-
H (at%)	<5	5–50	<5	5–50	40–70
Deposition method	PVD	PVD, CVD, PVD + CVD	PVD	CVD, PVD + CVD	CVD, PVD
Deposition temperature (°C)	RT-300	RT-500	RT-200	RT-500	RT-100
True density ρ (g/cm^3) (as reference)	3.5 > ρ > 2.6	2.6 > ρ > 2.0	1.7 > ρ > 1.4	2.0 > ρ > 1.4	ρ < 1.4
Coefficient of friction vs. steel (dry cond.) (as reference)	0.1–0.2	0.08–0.2	0.1–0.2	0.08–0.2	Unstable
Wear resistance vs. steel (dry cond.)	A	B–A	C	B–A	×
Nano-indentation hardness (H_{IT}: GPa)	25–90	9–35	9–25	9–25	0.5–9
Young's modulus (GPa)	200–900	120–300	100–400	100–220	~100
Corrosion resistance	B–A	C–B	×–C	B	B
Water contact angle (°) (as reference)	70–80	80–100	70–100	70–90	~70
Refractive index *n* (λ = 550 nm)	2.5–3.0	2.0–2.5	1.8–2.5	1.7–2.4	1.5–2.0
Extinction coefficient *k* (λ = 550 nm)	0.04–0.5	0.05–0.6	0.1–0.6	0.05–0.6	~0.1

Classification	DLC	DLC	DLC	DLC	not DLC
Color (500 nm in thick)	Transparent (Interference color)	Brown	Black	Light brown	Transparent
Optical band gap (eV)	0.2–1.7	1.0–2.5	1.0–1.7	0.5–2.0	NA

A: Excellent; B: Good; C: Somewhat poor; ×: Poor; NA: Unknown.

carbon.

3. McKenzie, D.R. Tetrahedral bonding in amorphous carbon. Rep. Prog. Phys. 1996, 59, 1611–1664.
4. Erdemir, A.; Donnet, C. Tribology of diamond-like carbon films: Recent progress and future prospects. J. Phys. D Appl. Phys. 2006, 39, R311.
5. Aisenberg, S.; Chabot, R. Ion-beam deposition of thin films of diamondlike carbon. J. Appl. Phys. 1971, 42, 2953–2958.
6. Gupta, B.K.; Bhushan, B. Micromechanical properties of amorphous carbon coatings deposited by different deposition techniques. Thin Solid Film. 1995, 270, 391–398.
7. Neuville, S. New application perspective for tetrahedral amorphous carbon coatings. Sci. Connect. 2014, 8, 1–27.
8. Donnet, C.; Fontaine, J.; Le Mogne, T.; Belin, M.; Heau, C.; Terrat, J.P.; Vaux, F.; Pont, G. Diamond-like carbon-based functionally gradient coatings for space tribology. Surf. Coat. Technol. 1999, 120–121, 548–554.
9. Kano, M. Super low friction of DLC applied to engine cam follower lubricated with ester-containing oil. Tribo. Int. 2006, 39, 1682–1685.
10. Weiler, M.; Sattel, S.; Jung, K.; Ehrhardt, H.; Veerasamy, V.S.; Robertson, J. Highly tetrahedral, diamond-like amorphous hydrogenated carbon prepared from a plasma beam source. Appl. Phys. Lett. 1994, 64, 2797–2799.
11. Angus, J.C.; Jansen, F. Dense "diamondlike" hydrocarbons as random covalent networks. J. Vat. Sci. Technol. 1988, A 6, 1778–1782.
12. Angus, J.C. Diamond and diamond-like films. Thin Solid Film. 1992, 216, 126–133.
13. Jacob, W.; Muller, W. On the structure of thin hydrocarbon films. Appl. Phys. Lett. 1993, 63, 1771–1773.
14. Bewilogua, K.; Hofmann, D. History of diamond-like carbon films—From first experiments to worldwide applications. Surf. Coat. Technol. 2014, 242, 214–225.
15. Reinke, P.; Jacob, W.; Möller, W. Influence of the ion energy on the growth and structure of thin hydrocarbon films. J. Appl. Phys. 1993, 74, 1354–1361.

16. Zhang, L.; Wei, X.; Lin, Y.; Wang, F. A ternary phase diagram for amorphous carbon. Carbon 2015, 94, 202–213.
17. Vetter, J. 60 years of DLC coatings: historical highlights and technical review of cathodic arc processes to synthesize various DLC types, and their evolution for industrial applications. Surf. Coat. Technol. 2014, 257, 213–240.
18. Robertson, J. Diamond-like carbon. Pure Appl. Chem. 1994, 66, 1789–1796.
19. Ferrari, A.C.; Robertson, J. Raman spectroscopy of amorphous, nanostructured, diamond-like carbon, and nanodiamond. Philos. Trans. R. Soc. Lond. 2004, A 362, 2477–2512.
20. Erdemir, A. The role of hydrogen in tribological properties of diamond-like carbon films. Surf. Coat. Technol. 2001, 146–147, 292–297.
21. Hirakuri, K.K.; Minorikawa, T.; Friedbacher, G.; Grasserbauer, M. Thin film characterization of diamond-like carbon films prepared by r.f. plasma chemical vapor deposition. Thin Solid Film. 1997, 302, 5–11.
22. Caschera, D.; Cossari, P.; Federici, F.; Kaciulis, S.; Mezzi, A.; Padeletti, G.; Trucchi, D. Influence of PE-CVD parameters on the properties of diamond-like carbon films. Thin Solid Film. 2001, 519, 4087–4091.
23. Isono, Y.; Namazu, T.; Terayama, N.; Tanaka, T. Mechanical characterization of sub-micrometer Thick DLC Films by AFM Tensile Testing for Surface Modification in MEMS. Proc. IEEE Micro Electro. Mech. Syst. 2002, 431–434.
24. Kim, Y.T.; Cho, S.M.; Choi, W.S.; Hong, B.; Yoon, D.H. Dependence of the bonding structure of DLC thin film on the deposition condition of PECVD method. Surf. Coat. Technol. 2003, 169, 291–294.
25. Nakahigashi, T.; Tanaka, Y.; Miyake, K.; Oohara, H. Properties of flexible DLC film deposited by amplitude-modulated RF P-CVD. Tribo. Int. 2004, 37, 907–912.
26. Ohtake, N.; Saito, T.; Kondo, Y.; Hosono, S.; Nakamura, Y.; Imanishi, Y. Synthesis of Diamond-like Carbon Films by Nanopulse Plasma Chemical Vapor Deposition at Subatmospheric Pressure. Jpn. J. Appl. Phys. 2004, 43, L1406–L1408.
27. Ohana, T.; Nakamura, T.; Suzuki, M.; Tanaka, A.; Koga, Y. Tribological properties and characterization of DLC films deposited by pulsed bias CVD. Diam. Relat. Mater. 2004, 13, 1500–1504.
28. Nakanishi, K.; Mori, H.; Tachikawa, H.; Itou, K.; Fujioka, M.; Funaki, Y. Investigation of DLC-Si coatings in large-scale production using DC-PACVD equipment. Surf. Coat. Technol. 2006, 200, 4277–4281.

29. Fujimoto, S.; Ohtake, N.; Takai, O. Mechanical properties of silicon-doped diamond-like carbon films prepared by pulse-plasma chemical vapor deposition. Surf. Coat. Technol. 2011, 206, 1011–1015.
30. Seker, Z.; Ozdamar, H.; Esen, M.; Esen, R.; Kavak, H. The effect of nitrogen incorporation in DLC films deposited by ECR Microwave Plasma CVD. Appl. Surf. Sci. 2014, 314, 46–51.
31. Chen, J.Y.; Wang, L.P.; Fu, K.Y.; Huang, N.; Leng, Y.; Leng, Y.X.; Yang, P.; Wang, J.; Wan, G.J.; Sun, H.; et al. Blood compatibility and sp3/sp2 contents of diamond-like carbon (DLC) synthesized by plasma immersion ion implantation-deposition. Surf. Coat. Technol. 2002, 156, 289–294.
32. Flege, S.; Hatada, R.; Ensinger, W.; Baba, K. Improved adhesion of DLC films on copper substrates by preimplantation. Surf. Coat. Technol. 2014, 256, 37–40.
33. Hiratsuka, M.; Nakamori, H.; Kogo, Y.; Sakurai, M.; Ohtake, N.; Saitoh, H. Correlation between Optical Properties and Hardness of Diamond-Like Carbon Films. Solid Mech. Mater. Eng. 2013, 7, 187–198.
34. Bewilogua, K.; Wittorf, R.; Thomsen, H.; Weber, M. DLC based coatings prepared by reactive d.c. magnetron sputtering. Thin Solid Film. 2004, 447–448, 142–147.
35. Chen, S.-Y.; Ou, K.-L.; Huang, W.-C.; Chu, K.-T.; Ou, S.-F. Phase transformation of diamond-like carbon/silver composite films by sputtering deposition. Ceram. Int. 2013, 39, 2575–2580.
36. Fujimaki, S.; Kashiwase, H.; Kokaku, Y. New DLC coating method using magnetron plasma in an unbalanced magnetic field. Vacuum 2000, 59, 657–664.
37. Amanovn, A.; Watabe, T.; Tsuboi, R.; Sasaki, S. Fretting wear and fracture behaviors of Cr-doped and non-doped DLC films deposited on Ti–6al–4V alloy by unbalanced magnetron sputtering. Tribo. Int. 2013, 62, 49–57.
38. Kamijo, E.; Nakamura, T.; Tani, Y. AFM observations of DLC films prepared by the ECR sputtering method. Nucl. Instr. Methods Phys. Res. 1997, B 121, 110–115.
39. Pang, J.; Lu, W.; Xin, Y.; Wang, H.; He, J.; Xu, J. Plasma Diagnosis for Microwave ECR Plasma Enhanced Sputtering Deposition of DLC Films. Plasma Sci. Technol. 2012, 14, 172–176.
40. Münz, W.-D.; Schenkel, M.; Kunkel, S.; Paulitsch, J.; Bewilogua, K. Industrial Applications of HIPIMS. J. Phys. Conf. Ser. 2008, 100, 082001.
41. Evaristo, M.; Fernandes, F.; Cavaleiro, A. Room and High Temperature Tribological Behaviour of W-DLC Coatings Produced by DCMS and Hybrid DCMS-HiPIMS Configuration. Coatings 2020, 10, 319.
42. Xu, S.; Tay, B.K.; Tan, H.S.; Zhong, L.; Tu, Y.Q.; Silva, S.R.P.; Milne, W.I. Properties of carbon ion deposited tetrahedral amorphous carbon films as a function of ion energy. J. Appl. Phys. 1996,

79, 7234–7240.

43. Inaba, H.; Fujimaki, S.; Sasaki, S.; Hirano, S.; Todoroki, S.; Furusawa, K.; Yamasaka, M.; Shi, X. Properties of Diamond-Like Carbon Films Fabricated by the Filtered Cathodic Vacuum Arc Method. Jpn. J. Appl. Phys. 2002, 41, 5730–5733.
44. Takikawa, H.; Izumi, K.; Miyano, R.; Sakakibara, T. DLC thin film preparation by cathodic arc deposition with a super droplet-free system. Surf. Coat. Technol. 2003, 163–164, 368–373.
45. Kondo, S.; Liza, S.; Ohtake, N.; Akasaka, H.; Matsuo, M.; Iwamoto, Y. Mechanical characterization of segment-structured hydrogen-free a-C films fabricated by filtered cathodic vacuum arc method. Surf. Coat. Technol. 2015, 278, 71–79.
46. Weissmantel, C.; Reisse, G. Preparation of hard coatings by ionbeam methods. Thin Solid Film. 1979, 63, 315–325.
47. Akita, N.; Konishi, Y.; Ogura, S.; Imamura, M.; Hu, Y.H.; Shi, X. Comparison of deposition methods for ultra thin DLC overcoat film for MR head. Diam. Relat. Mater. 2001, 10, 1017–1023.
48. Roy, R.K.; Ahmed, S.F.; Yi, J.W.; Moon, M.-W.; Lee, K.-R.; Jun, Y. Improvement of adhesion of DLC coating on nitinol substrate by hybrid ion beam deposition technique. Vacuum 2009, 83, 1179–1183.
49. Oohira, K. Characteristics and Applications of DLC films. NTN Tech. Rev. 2009, 77, 90–95.
50. Lan, R.; Ma, Z.; Wang, C.; Lu, G.; Yuan, Y.; Shi, C. Microstructural and tribological characterization of DLC coating by in-situ duplex plasma nitriding and arc ion plating. Diam. Relat. Mater. 2019, 98, 107473.
51. Panda, M.; Krishnan, R.; Krishna, N.G.; Amirthapandian, S.; Magudapathy, P.; Kamruddin, M. Tuning the tribological property of PLD deposited DLC-Au nanocomposite thin films. Ceram. Int. 2019, 45, 8847–8855.
52. Scheibe, H.-J.; Schultrich, B. DLC film deposition by Laser-Arc and study of properties. Thin Solid Film. 1994, 246, 92–102.
53. Wu, J.-B.; Chen, C.-Y.; Shin, C.-T.; Li, M.-Y.; Leu, M.-S.; Li, A.-K. Microstructure and physical properties of DLC films deposited by laser induced high current pulsed arc deposition. Thin Solid Film. 2008, 517, 1141–1145.
54. VDI 2840 Carbon Films—Basic Knowledge, Film Types and Properties; Verein Deuttscher Ingennieure: Dusseldorf, Germany, 2005.
55. Takabayashi, S.; Okamoto, K.; Shimada, K.; Motomitsu, K.; Motoyama, H.; Nakatani, T.; Sakaue, H.; Suzuki, H.; Takahagi, T. Chemical Structural Analysis of Diamondlike Carbon Films with Different Electrical Resistivities by X-ray Photoelectron Spectroscopy. Jpn. J. Appl. Phys. 2008, 47, 3376–3379.

56. Wang, S.; Dong, Y.; He, C.; Gao, Y.; Jia, N.; Chen, Z.; Song, W. The role of sp2/sp3 hybrid carbon regulation in the nonlinear optical properties of graphene oxide materials. RSC Adv. 2017, 7, 53643–53652.